

# Technical Note: Calibration-Free pH Sensing of Ocean and Estuarine Waters

Monica Miranda Mugica<sup>1</sup>, Christina Day<sup>1</sup>, Brandon McHale<sup>1</sup>, Kay L. McGuinness<sup>1</sup>, Gareth Lee<sup>2</sup>, Daisy Pickup<sup>2</sup>, Nathan S. Lawrence<sup>1</sup>

5 <sup>1</sup> ANB Sensors Ltd., 4 Penn Farm, Haslingfield Cambridge, CB23 1JZ, UK

<sup>2</sup> School of Environmental Sciences, University of East Anglia, Norwich Research Park, Norwich, NR4 7TJ, UK

*Correspondence to:* Nathan S. Lawrence (nlawrence@anbsensors.com)

**Abstract.** An electrochemical based, all solid-state, calibration-free pH sensor is presented. The sensor is targeted for monitoring the pH of ocean and estuarine environments covering a salinity range from 10-35 PSU without the need for any salinity measurements. The sensor performance is demonstrated in both laboratory and field conditions, showing a pH of 8.33 in two sensors, against a pH of 8.34 of a freshly calibrated glass pH sensor. Excellent precision is also shown, exhibiting a pH of 8.33 +/- 0.015 and 8.33 +/- 0.012 across multiple measurements. The field tests were conducted in an estuarine environment close to Oban in Scotland where the sensor was deployed for a period of three days. The sensor was validated against a sampled solution that measured a pH of 7.74, which was equivalent to the pH 7.74 obtained from ANB's pH sensor at that exact time, and it was tested alongside a glass pH sensor during deployment, demonstrating its stability over 3 days of testing. The data highlighted the ability of the sensor to monitor the tidal variations of pH in the estuarine environment.

## 1 Introduction

The measurement of pH in the world's oceans is extremely important and is indispensable to researchers, industrialists, legislators and government organisations to provide an understanding of the ocean's health. The health of the ocean is impacted by various events such as pollution through industrial outfalls and environmental disasters, its absorption of CO<sub>2</sub> from the atmosphere, or through naturally occurring events such as the release of gases through subsea vents.

pH is a major factor in the effluent treatment process and its monitoring throughout the process from start to outfall is extremely important in ensuring the effectiveness and performance of the process, regardless of the nature of the treatment - physical, chemical or biological (Dai et al., 2015b; pH, 2017).

Ocean acidification is a significant and unfavourable consequence of the excess carbon dioxide (CO<sub>2</sub>) in the atmosphere. Prior to the industrial revolution, carbon dioxide concentrations varied between 180 and 300 ppmv. However, today's atmospheric CO<sub>2</sub> concentration is 380 ppmv and increasing ~0.5 % per year. In the past 200 years, the world's oceans have become almost 30 % more acidic (Siegenthaler et al, 2017; Sabine et al, 2004). Water reacts with CO<sub>2</sub> to form carbonic acid (H<sub>2</sub>CO<sub>3</sub>), releasing

hydrogen ions ( $H^+$ ), (Barker and Ridgwell, 2012), causing the solution pH to decrease. Previously it was believed that dissolved chemicals carried by the rivers to the ocean were enough to keep the ocean's pH stable and so the impact of rising  $CO_2$  levels would be negated. However, the rate of dissolution of carbon dioxide into the ocean is so rapid, that the natural buffering effect has been overwhelmed, resulting in a rapid decrease of ocean pH (Bennett, 2018). If the world's oceans carry on absorbing  $CO_2$  at their current rates, average global ocean surface pH is expected to drop to 7.8 or 7.7 by the end of this century creating the most acidic ocean for the past 20 million years (Caldeira and Wicket, 2005).

A secondary issue caused by ocean acidification is the lower abundance of carbonate ions, which is key to organisms like corals or mussels to build shell and skeletons (NOAA, 2020; Fabry, 2018). Many chemical reactions are sensitive to small changes in pH which can have detrimental effects on marine life, affecting reproduction and growth (Doney et al., 2009). This is a key reason why pH is one of the most important ocean water quality parameters (Hickin, 1995).

Excess carbon dioxide in the atmosphere, is causing higher ambient temperatures, especially in the poles, where many glaciers are now rapidly melting. These melting glaciers impact ocean currents and rises sea levels. If  $CO_2$  discharge continues to increase, the current rate of melting ice is expected to double by the end of the century, and Antarctic melt alone will raise the global sea level by 5 feet (Hancock, 2022; Stone, 2021).

Alteration of the ocean environment is not only occurring through manmade events, but also through natural events such as subsea geologic formations where  $CO_2$  is naturally escaping through the seafloor (e.g., hydrothermal vents). These can be difficult to detect and vary with factors such as bathymetry, hydrography, and magnitude and type of the leakage. pH is an excellent proxy for monitoring  $CO_2$  levels around these vents (Botnen et al., 2015; Downing, 2014).

Today ocean pH sensors are focused on potentiometry or spectrophotometry (Martz et al., 2015). Potentiometry encompasses two key technologies: glass pH probes and ion sensitive field effect transistors (ISFETs). The glass pH probe is one of the most common sensors however, although special ocean glass probes are available (SeaBed, 2021; Sea & Sun, 2021), they are problematic when deployed in the ocean. They suffer from reference electrode drift, caused by changes in the environment of the reference chamber, so therefore require frequent recalibrations. They have to be kept under special storage conditions to try and keep the reference chamber uncontaminated, and, as they are made from glass, they often suffer fragility issues. ISFET technologies are much more robust than their glass analogues and sensors have been developed specifically for the ocean environment (Shitashima et al., 2002; Takeshita et al., 2014; Johnson et al., 2016; Briggs et al., 2017; [21] Kremesti, 2021). However, they still suffer from reference drift and they often have to be deployed with salinity sensors to understand reference potentials. They also face other challenges like light sensitivity and drift when multiple sensor types are co-located (Bresnahan Jr et al., 2014; Jimenez-Jorquera and Baldi, 2010; Martz et al., 2010). Spectrophotometric based systems don't suffer from

reference drift and provide very accurate pH readings (Clayton and Byrne, 1993; Seidel et al., 2008; Rerolle et al., 2013; DeGrandpre et al., 2014). However, deployment issues around maintenance remain because of their need to mix the pH indicator dye with a seawater sample. This means they require deployment with optical dye bags which need to be replaced periodically and flowlines which can be blocked by biofouling species (Newhall et al., 2007; Rerolle et al., 2016; Chen et al., 2010).

Small changes in pH value can equate to much larger variations in practice, as a small drift can have a significant effect on product quality as well as process efficiency and safety. When referring to accurate pH values, it is important to note that the accuracy needed depends on the final application. For instance, for the research of the ocean acidification, a  $\pm 0.05$  pH units accuracy is required, while for aquaculture or aquarium management, as well as for general water and wastewater treatments, an accuracy of  $\pm 0.1$  pH units, will suffice.

In this paper, a new technology that exhibits several advantages from the technologies described above is presented. This relies on a redox active/pH active molecule that is combined with a redox active/pH inactive molecule to determine the pH of the seawater without the need of a calibration (Lu and Compton, 2014). The main advantage of this novel technology is that any reference drift is tracked and accounted for in-situ, so it does not require any calibration. Moreover, the sensor does not require any special storage conditions and can be left dry, allowing for pH to be monitored in places where this has never been done before, such as flood plain and tidal monitoring.

## **2. Experimental**

### **2.1 Laboratory Tests**

Laboratory tests were conducted in temperature controlled stirred solutions. The solution was produced using synthetic sea salts (H2Ocean Natural Reef Salt, purchased from Maidenhead Aquatics, UK) diluted to the correct concentration using deionised water. CO<sub>2</sub> (BOC, 99%) was bubbled into the solution periodically to manipulate the pH. Temperature control was obtained through a temperature exchange loop placed inside a temperature-controlled chamber. The exchange loop temperature was manipulated through an external temperature-controlled bath (Fisher Scientific Isotemp 4100 R20 Refrigerated/Heated Bath Circulator) and held at 15°C for the time of the experiment. The solution was stirred using a Teflon overhead stirrer and the temperature measured using a k type thermocouple sheathed in polymer housing. The sensors were immersed in the tank and connected to a control unit via a SubConn cable. The sensors were powered using a 12 V battery supply and each sensor used was switched on and off during the course of the experiment to ensure there was no bias in the experiment. The solution was sampled periodically throughout the course of the experiment and the pH measured using a glass ocean pH probe which was daily calibrated using pH 4, pH 7 and pH 10 standard buffers.

This experimental set up is only for Sect 4 'Results and Discussion'.

2.2 Field Trials

The sensor was tested in Ardmucknish bay, located in Dunbeg, a village located outside Oban, Scotland (Figure 1). Ardmucknish bay is a wide-open, south facing bay, opposite to the island of Mull.

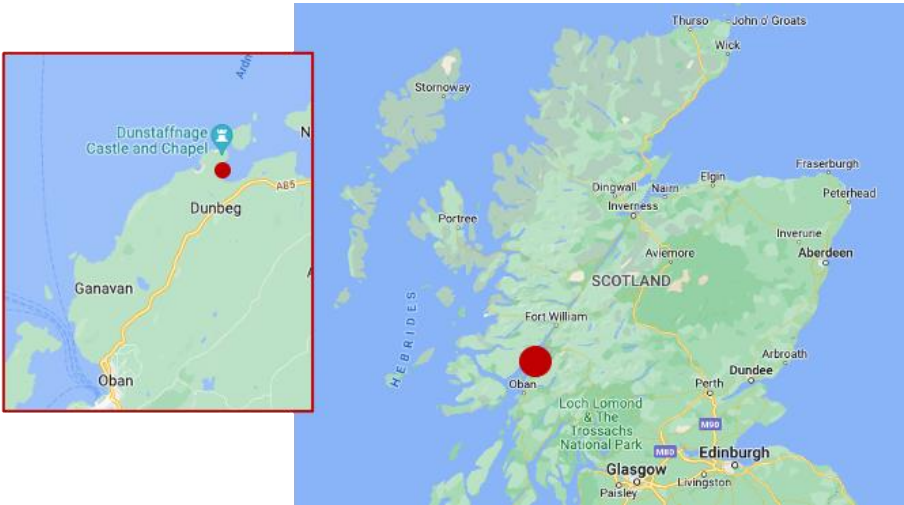
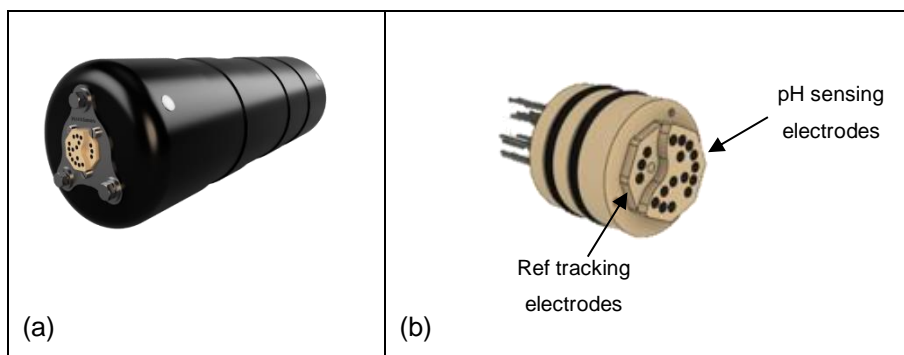


Figure 1: Sensor testing location: Ardmucknish bay, Dunbeg, Scotland.

© Google Maps

3 Technology

To overcome the drawbacks of today’s pH sensing devices an innovative approach is presented encompassing a solid-state, calibration-free sensor. The sensor has been developed to be plug and play to the end user, with little maintenance and no need for regular factory recalibrations. It has a range of 2-10 pH units and an accuracy of +/- 0.05 pH units. Figure 2 shows the image of the sensor with the sensing element, or transducer, at the front end. This transducer is a replaceable part which can be easily replaced when required (vide infra), whilst the back end utilises a submersible connector through which power and communications are passed to the control unit. On board the sensor is the electronic circuitry required to control the sensor and convert the raw measurement signal to the solution pH in a timestamped manner to the end user.



**Figure 2:** (a) The mechanical housing of the sensor including the transducer. (b) An image of the transducer depicting the recessed reference tracking electrodes and the pH sensing electrodes on the front face.

### 3.1 Transducer

This innovative calibration-free pH sensor is based on a voltammetric electrochemical technique, where a time-dependent potential is applied to each electrode in the transducer and the resulting current is measured as a function of that potential (Bard, 2000). The pH is calculated using the resulting peak potential, as it is linearly associated with the pH. The sensor utilizes a pH active molecule combined with a pH inactive molecule within a solid-state matrix. 2'-hydroxyflavanone is used as the electroactive polymer for the pH sensing part (Miranda, 2022), and anthraquinone – modified carbon electrode (Sisodia, 2022) as the pH insensitive sensor. The electrochemical response of both species can determine the pH of the seawater with no need for calibration, by tracking the performance of the reference electrode (pH inactive molecule) through an additional in-situ electrochemical measurement (Dai et al., 2015a). As mentioned, the peak potential of the pH sensing electrodes moves with pH, allowing the determination of pH. At the same time, the pH inactive electrode tracks the reference drift, and therefore, generates a calibration free pH measurement. Figure 3 shows how the peak potential shifts to lower potentials as the pH of the solution increases for the pH sensing electrodes (Figure 3A) whilst the reference tracker potential stays stable (Figure 3B), only changing in peak position when the reference is drifting. Figure 3 was obtained by testing both pH sensing and reference trackers in synthetic seawater (H2Ocean Natural Reef Salt, Maidenhead Aquatics, UK). The pH of the solution was decreased by the addition of CO<sub>2</sub>, allowing the response of both the pH sensing and reference sensing elements to be monitored. The pH was measured using a full ocean glass pH probe (Idronaut, Italy), which it was calibrated using standard buffers. When the pH sensing electrodes and reference tracker are combined, subtracted values can be calculated, and based on the calibration algorithm shown in Fig. 3C, the resulting pH can be determined. The calibration of the sensor shows a sensitivity of 54.8 mV/pH unit in synthetic seawater, overlaying the calibration plot obtained for pH 4, pH 7 and pH 9 IUPAC standard buffers, with a sensitivity of 56.5 mV/pH unit [1] [10] (Miranda Mugica et al., 2022)

145

150

155

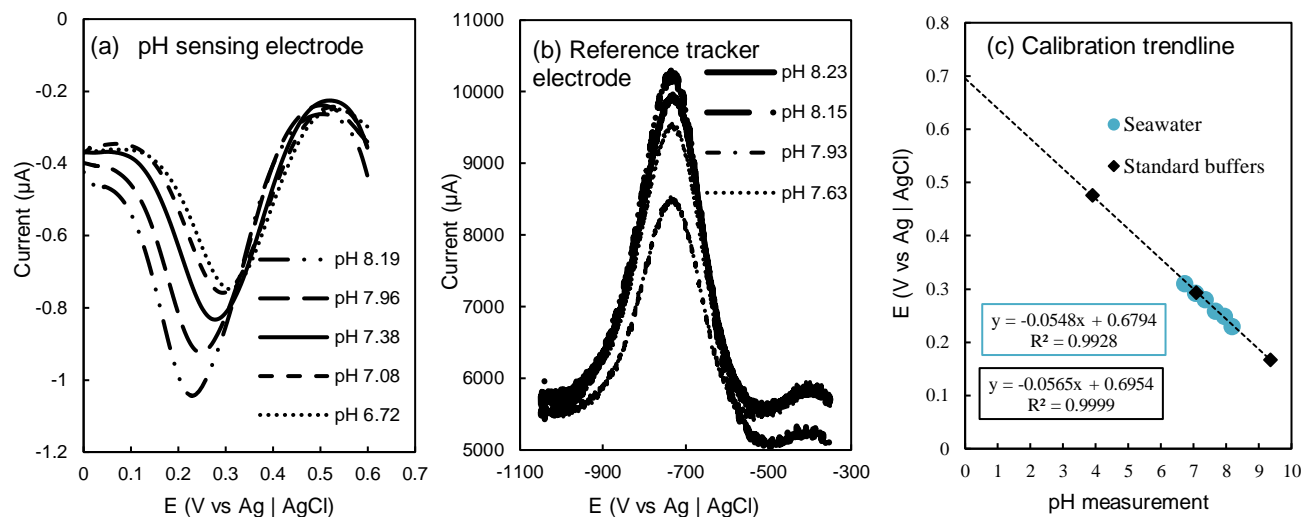


**Figure 3:** The voltammetric response collected by the sensor for both (a) the pH sensing (frequency=100 Hz, step potential=1 mV, amplitude=40 mV) and (b) the reference tracker electrodes (frequency=300 Hz, step potential=0.5 mV, amplitude=80 mV) in synthetic seawater/CO<sub>2</sub> system, and (c) the resulting calibration trendline in synthetic seawater and IUPAC standard buffers, using the subtracted values. pH values were measured using a calibrated glass pH probe.

160

165

The efficacy of this approach is shown in Figure 4, where the sensor was deployed in a temperature-controlled seawater tank, at 293K. Figure 4A details the variation in peak potential of both the pH sensing and reference tracking systems as a function of time. After 10 h of deployment, a large change in peak potential was observed in the pH sensing system. Nevertheless, the reference tracker exhibited the same change in potential, meaning that the Ag/AgCl redox couple was impacted due to a change in the environment of the reference electrode. The tracking of the reference electrode allows the system to correct the internal drift of the reference electrode. Figure 4B shows the end user result of pH as a function of time, displaying a pH 8.07  $\pm$  0.039 over a 14 h experiment, highlighting the robustness of the sensing system where no change is seen in the pH measurement owing to the reference electrode tracker correction, with no need of re-calibration. Without the reference tracker this phenomenon may be wrongly attributed to a pH change by the end user.

170

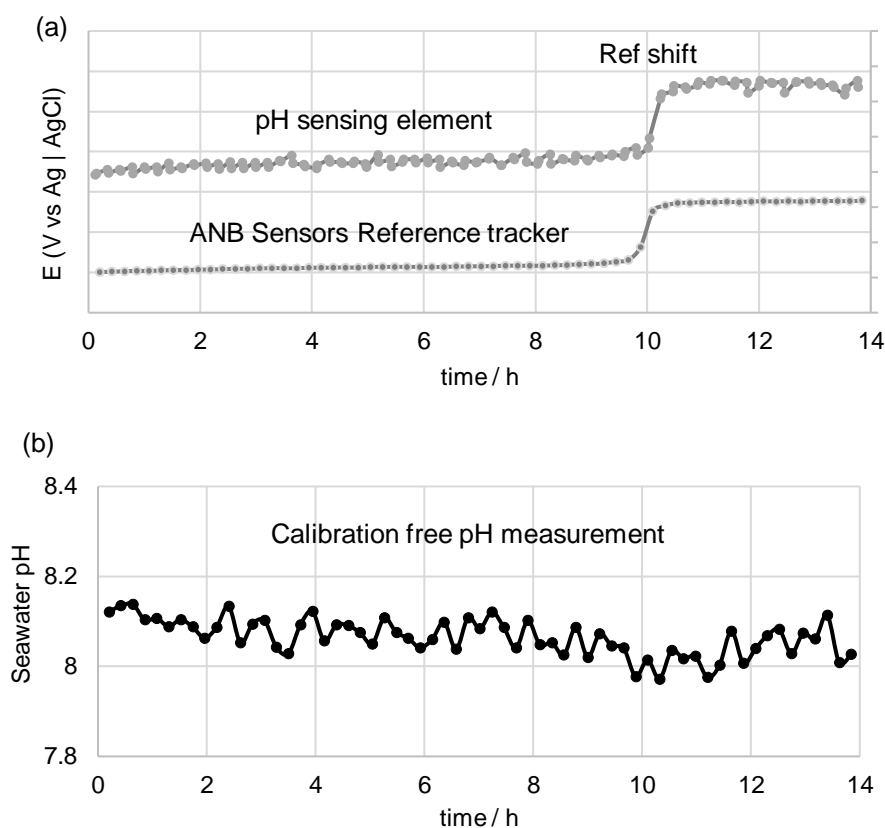
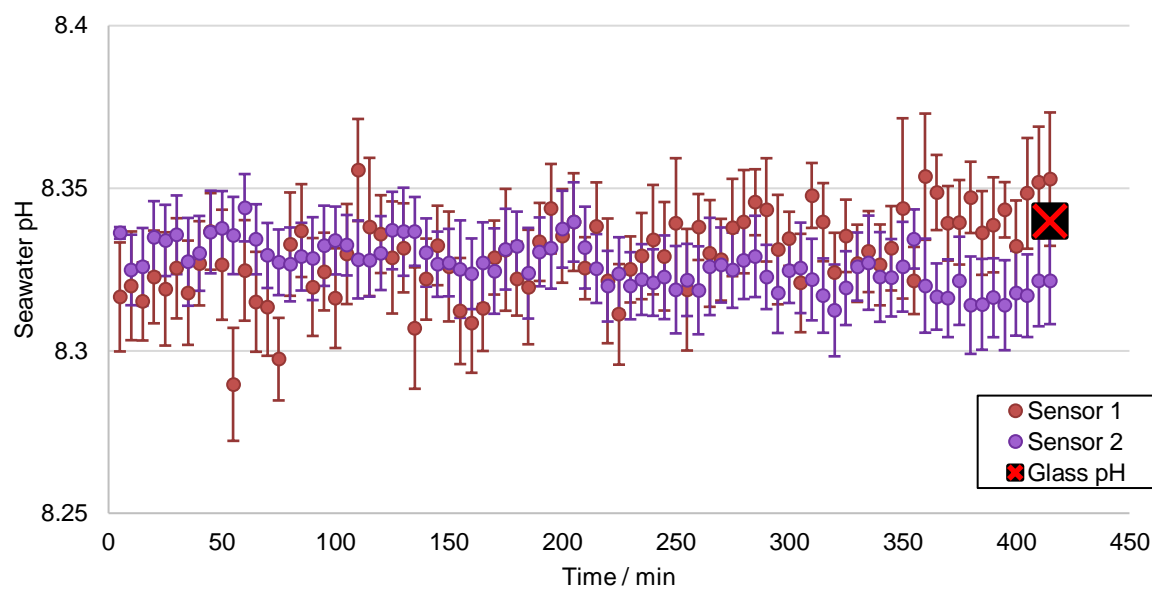


**Figure 4:** (a) The plot of peak potential for the reference tracking and pH sensing elements as a function of time. (b) The final calibration free pH sensor output as a function of time.

Figure 5 shows the pH values obtained using two sensors tested simultaneously in synthetic seawater, in a temperature-controlled tank, (see section 2.1) at 288K, where using the recipe outlined provides a pH of 8.30 at 298K. The sensor scans the reference electrode first, to track any changes in the reference electrode potential, and then the twelve pH sensitive electrodes in the transducer head, taking ca.15 seconds for each pH measurement. Each data point represents the average of the twelve pH measurements over five minutes testing. This data shows the reproducibility of the two sensors taken in the same tank without any calibration prior to deployment. Across the entire set of measurements an average pH value of  $8.33 \pm 0.015$  and  $8.33 \pm 0.012$  for sensor 1 and sensor 2, respectively, were obtained. Without averaging the twelve pH measurements, the accuracy for each sensor was  $8.33 \pm 0.04$  and  $8.33 \pm 0.03$ . The data obtained is in an excellent agreement with the pH 8.34 measured by a freshly calibrated full ocean glass pH sensor as well as with the expected theoretical pH of the synthetic seawater. Even though glass pH electrodes suffer from reference drift and are not ideal for deployment conditions due to their

190 fragility, a one-point measurement can be trusted when freshly calibrated using standard buffers. For that reason, the accuracy of the sensor can be confirmed, along with the reproducibility across different systems.



195 **Figure 5:** Representation of pH values obtained by two sensors in synthetic seawater at a constant temperature, compared with the pH measured by a glass pH probe. Each measurement corresponds to the average of twelve pH measurements over five minutes testing.

**3.2 Lifetime and Maintenance**

200 The lifetime of the sensor is dependent on the number of measurements that each electrode records and not on the deployment time of the sensor. The electrodes in the transducer are repetitively cycled and the continual voltammetric measurements on each electrode decays the response of each electrode. This is seen through a loss in the voltammetric peak size until the peak potential can no longer be deciphered. At this point the sensor notifies the end-user maintenance is required. It is for this reason that there are a number of electrodes on the front surface of the transducer so as to maximise the lifetime of the sensor before  
205 maintenance is required.

The sensor has an onboard processor which applies the one-time voltammetric sweep parameters to the electrochemical reaction occurring at each electrode. The resulting current received at the electrode due to the electrochemical reaction is then recorded, the data is analysed to determine the potential at which maximum current flows, which is then used to calculate the



corresponding pH value. The response of each electrode is analysed after each measurement to ensure an accurate response is observed, when this is not the case the health number is increased, to alert the end user that maintenance is required.

Maintenance of the sensor is through an abrasion of the transducer surface using an abrasion block (wet and dry paper, 320 grade). After the abrasion the sensor can be redeployed, and the health of the sensor returns to its original value. The transducer displays up to 15,000 measurements between abrasions and will last for approximately 25-30 abrasions before it will need replacing. The sensor has been designed so that the replacement of the transducer is very simple for the end user.

3.3 Electronics and Communication

The sensor operates in either autonomous (stand-alone) or user-controlled mode through an RS232/485 communication protocol. In autonomous mode the sensor is connected to a power source and operates at a pre-set measurement rate. The maximum frequency for displaying a pH reading is approximately 15 sec, with the possibility of decreasing the measurement rate depending on the end user requirements. The data is saved to an SD card and can be downloaded after deployment through a data retrieval unit via a USB connection to a PC.

In user-controlled mode the user defines the measurement rate and initiates the scan and shutdown commands. The data is returned to the control unit in real time. Table 1 summaries the supply voltage and current draw when the sensor is in various modes.

Table 1: A summary of the supply voltage and power consumption of the sensor.

Supply Voltage	External	6.5 to 20 VDC
Power Consumption	Sampling	ca. 110 mA
	Sleep	5 mA
On board Storage		8 GB

The pH output is calculated using an inbuilt algorithm based on the equation presented in Fig. 3C ( $y = -0.0548x + 0.6794$  where  $x$  corresponds to pH and  $y$  to the peak potential (V)), which combines a knowledge of the peak potential of both the pH sensing and reference tracking elements. As mentioned before, a potential is applied to each electrode and the resulting current

is measured as a function of that potential, obtaining the resulting voltametric response, which will provide the peak potential value needed for the calculation of the pH. Temperature is also needed for the algorithm to calculate the pH. The temperature is measured using the onboard k type thermocouple. An example of the sensor output is shown in Fig. 6. After the system details (firmware version, serial number, date, time, scanning mode) the sensor outputs the date/time, pH, electrode number, temperature and health. As mentioned above, the health of the electrode corresponds to its condition and varies from 0 to 9. When the health of the majority of electrodes reaches 9, the transducer will require an abrasion.

```
*****
ANB SENSORS
Interface Firmware Version : V11.3
Driver Firmware Version   : V7.0
System Serial Number      : 000035
System Date (MM/DD/YY)    : 12/30/21
System Time (24 Hour)     : 10:05
System Style              : Controlled Scanning
Scanning Interval         : 15 Minutes
*****
scan
$ANB,05B8,0,000035,2021:12:30:10:06:02
$ANB,C40A,0,2021:12:30:10:07:26,$$.$$$,$$,12,281.300,3
$ANB,E0E8,0,2021:12:30:10:07:49,07.505,04,281.300,0
$ANB,9E0D,0,2021:12:30:10:08:12,07.476,08,281.300,0
$ANB,1AD4,0,2021:12:30:10:08:35,07.442,10,281.300,0
$ANB,707F,0,2021:12:30:10:08:57,07.409,02,281.300,3
$ANB,1803,0,2021:12:30:10:09:20,07.437,05,281.400,0
$ANB,E74D,0,2021:12:30:10:09:43,07.430,07,281.400,0
$ANB,9754,0,2021:12:30:10:10:06,07.470,09,281.400,0
$ANB,686C,0,2021:12:30:10:10:29,07.524,03,281.400,0
$ANB,00F2,0,2021:12:30:10:10:53,07.499,06,281.400,0
$ANB,2197,0,2021:12:30:10:11:16,07.481,11,281.400,0
```

**Time:** year:month:day:hour:minute:sec  
(e.g.: 2021:12:30:10:07:49)

**pH:** X.XXX  
(e.g.: 7.505)

**Electrode:** electrode from which pH is cycled  
(e.g.: 04)

**Temperature:** XXX.XXX K  
(e.g.: 281.300 K)

**Health:** Scaled from 0-9  
(e.g.: 0)

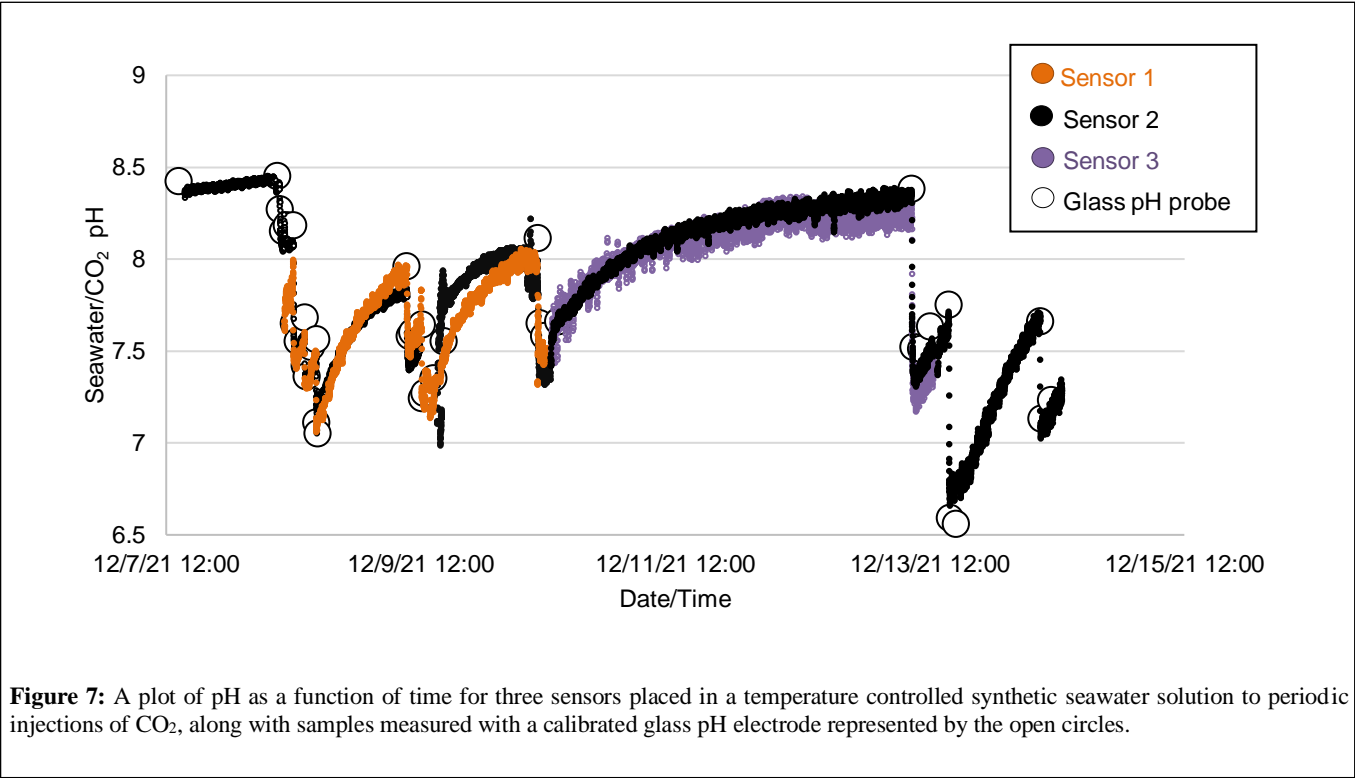
**Figure 6:** Sensor output from the terminal program.

4 Results and Discussion

4.1 Laboratory Testing

Testing of the sensor in the laboratory has focused on lifetime stability and the ability of the sensor to respond in real time to changes of pH in seawater solutions. Three different sensors were used to monitor the pH of a seawater solution for a week, and during this time CO<sub>2</sub> was sporadically bubbled into the solution to vary the pH, to pH 6.50, after which the seawater was left to degas between CO<sub>2</sub> injections. Figure 7 details the plot of pH as a function of time for all three sensors. Each individual electrode’s pH value has been presented instead of the average of the twelve, in order to improve the tracking of any small pH change. Initially only sensor 2 was tested, and after a day, sensor 1 was incorporated to the same seawater/CO<sub>2</sub> tank. Only two of the three sensors were tested in parallel at any one time: sensors 1 and 2 at the beginning, and sensor 3 was swapped with

sensor 1 during the course of the experiment. The data of the three sensors showed favourable agreement between them, confirming the reproducibility between the sensors. They reacted immediately to the pH changes, allowing the end user to detect any spontaneous pH change in the environment. The sensor's measured pHs were validated using a calibrated full ocean  
 260 pH sensor glass probe by measuring the pH of a small sample at certain times, assuming the efficacy of the glass pH probe after being freshly calibrated. The pH of the sensor and the glass pH probe can only be compared when the seawater was in a stable condition, i.e. before adding CO<sub>2</sub> or after letting degas completely. In the first test, before CO<sub>2</sub> was injected, sensor 2 presented a pH of 8.39 +/- 0.31 for all individual twelve electrodes over a day in seawater, while the glass pH probe measured a pH of 8.42 when freshly calibrated. The sensors result lay within the specifications outlined with respect to inter sensor  
 265 repeatability and even though the accuracy cannot be validated against the externally calibrated probe, it can be confirmed than the sensors follow the pH change correctly.



270 **Figure 7:** A plot of pH as a function of time for three sensors placed in a temperature controlled synthetic seawater solution to periodic injections of CO<sub>2</sub>, along with samples measured with a calibrated glass pH electrode represented by the open circles.

#### 4.2 Field Trials

The Field Trials were conducted over a period of three days (8<sup>th</sup> - 10<sup>th</sup> September 2021), with a pre-set delay time of 15 min.  
 275 between measurements. In this case the sensor was placed in autonomous mode, powered directly from a 12 V power supply with no interface control. The data was saved to the internal memory of the sensor and downloaded after deployment. Figure

8 details the data obtained from the sensor through a plot of pH variation (purple) and temperature (black) as a function of time over the 3 days. During the course of the trials, a water sample (ca. 250 mL) was taken in a plastic bottle and a pH of 7.73 was instantly measured using a calibrated glass pH electrode, which was equivalent to the pH 7.74  $\pm$  0.047 obtained from ANB's

280 pH sensor at that exact time. The pH of the sample was instantly measured in order to have the same temperature conditions as in the sea. The sensor presented a deviation of  $\pm$  0.048 pH units over the entire deployment, which is in accordance with the accuracy stated in the 'technical details' section. The data output from the sensor after 36 h of measuring on a 15 min measurement interval showed the semi-diurnal variations in pH ranging from 7.7 up to 7.9, consistent with the natural ebb and flow of the tidal waterways at Oban. At high tide, the river water mixes with the incoming seawater, producing a higher pH

285 value. The pH variation with tides was quite noticeable, a result of the high tidal coefficient in those 3 days. Tidal coefficients are referred to as the difference in water height between high and low tides, on a scale of 20 to 120. The sensor was deployed from the 8<sup>th</sup> - 10<sup>th</sup> September when high tidal coefficients - 101, 99 and 91 occurred (Oban, 2021). Being more specific, the tidal heights in those three days were 0.6 m and 4.3 m for low and high tides on the 8<sup>th</sup> of September, 0.7 m, 4.1 m, 0.6 m, and 4.3 m for the 9<sup>th</sup>, and 0.8 m and 4.1 m for the last day, 10<sup>th</sup> of September. All the tidal heights are referenced to the Mean

290 Lower Low Water (MLLW) point, which is the lowest of the two lowest tides per day in the last 19-year period. This phenomenon explains why such significant variations in pH were observed.

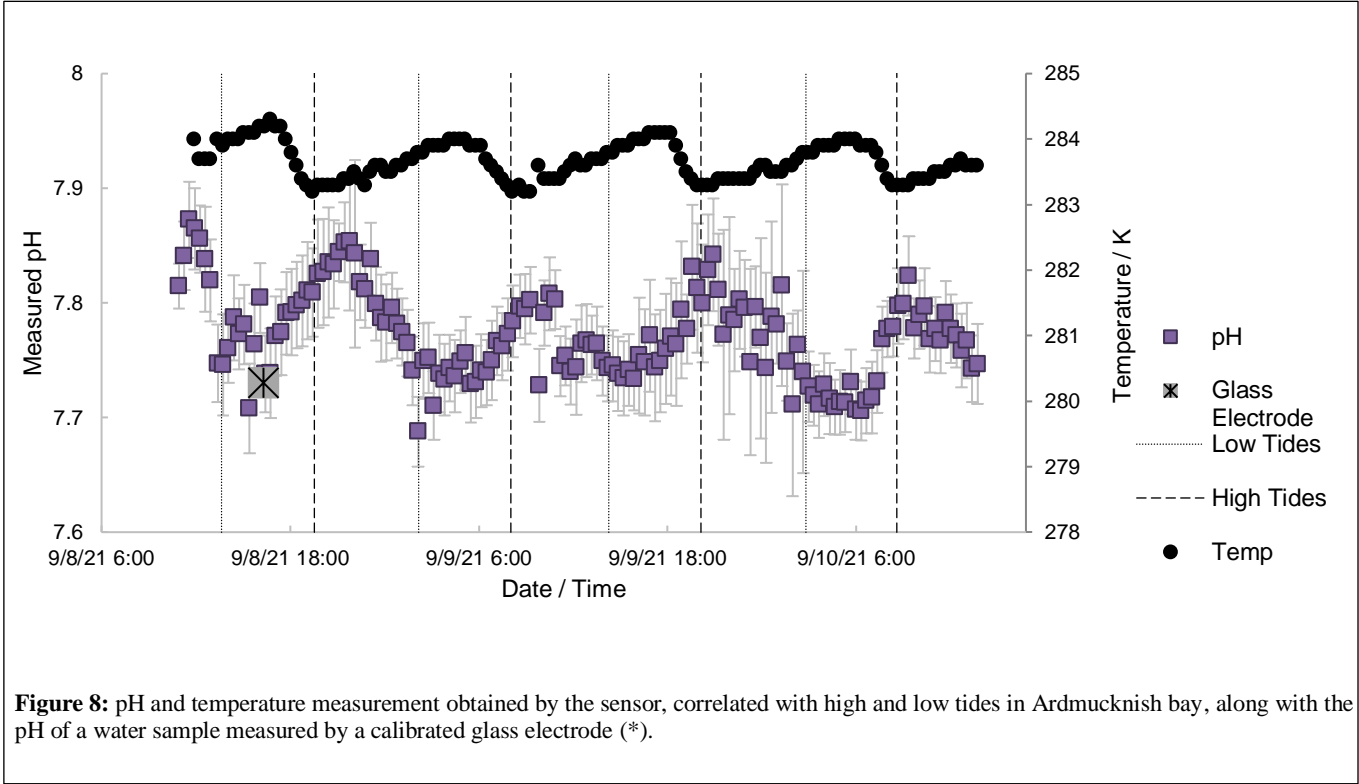


**Figure 8:** pH and temperature measurement obtained by the sensor, correlated with high and low tides in Ardmucknish bay, along with the pH of a water sample measured by a calibrated glass electrode (\*).

During the final day of the trial a glass electrode was deployed alongside the calibration free sensor. The corresponding data comparing the calibration free sensor's response to the glass electrode is shown in Figure 9. It can be clearly seen the glass electrode pH reading was unstable during the course of its deployment, with values ranging between 7.50 and 7.90 in pH, endorsing the advantage of using the calibration-free sensor against the glass electrode for deployment in sea water.

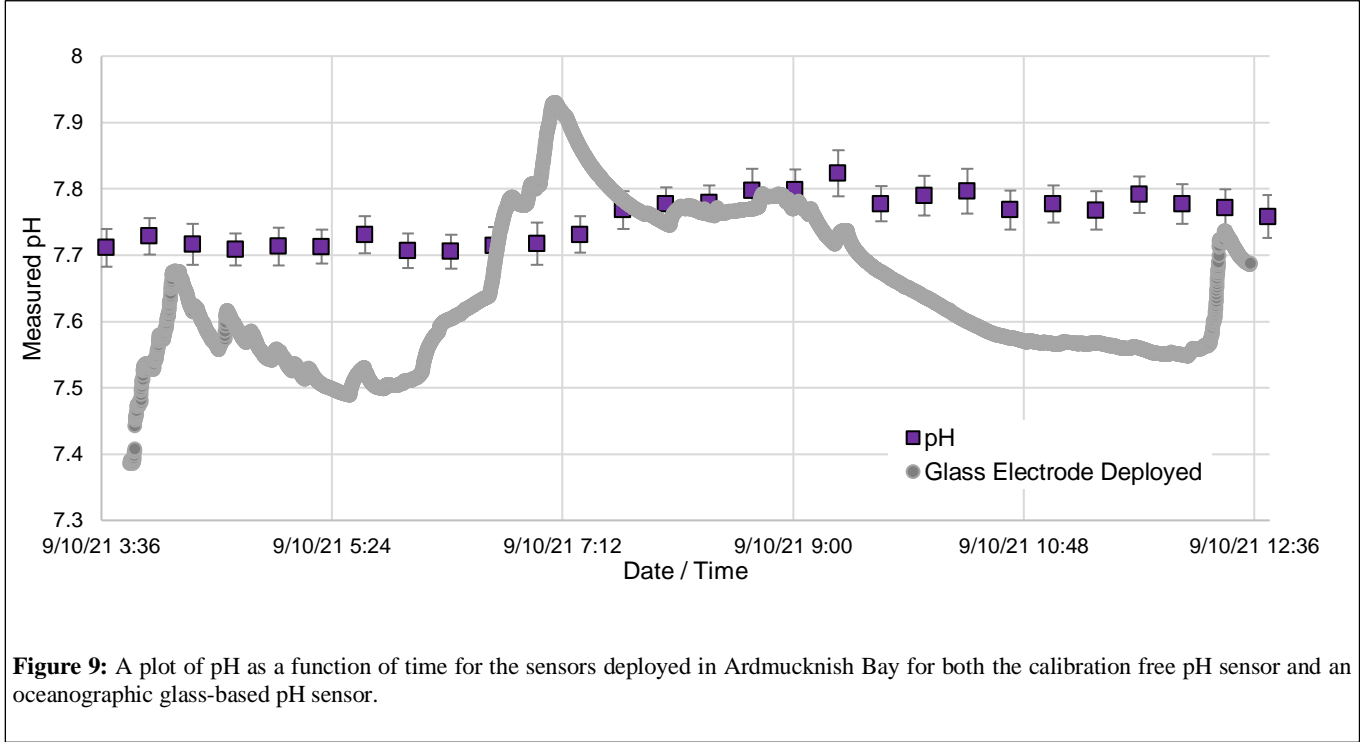


**Figure 9:** A plot of pH as a function of time for the sensors deployed in Ardmucknish Bay for both the calibration free pH sensor and an oceanographic glass-based pH sensor.

## 5. Conclusions

The results demonstrate the use of a new solid-state, calibration-free pH sensor in the monitoring of estuarine and ocean waters. The sensor was shown to respond effectively to pH in laboratory environments whereby the pH of the seawater solution was manipulated by the sporadic injection of CO<sub>2</sub> into the mixed solution. Sensors were run in conjunction to each other showing the inter reproducibility of the sensors and compared to a sample of solution whose pH was measured using a freshly calibrated full ocean glass electrode. Favourable agreement was observed throughout the seven-day experiment. The field trials were conducted in an estuarine environment close to Oban in Scotland where the sensor was deployed for a period of three days. The sensor was validated against a sampled solution and tested alongside a glass pH sensor system. The data highlighted the ability of the sensor to monitor the tidal variations of pH in the estuarine environment.

## Acknowledgements

320 This project has received funding from the European Union's Horizon 2020 research and innovation program under grant agreement No 82297. ANB Sensors gratefully acknowledges funding this work through Innovate UK grant funding, Grant no. 133171. Innovate UK is the UK's innovation agency. It works with people, companies and partner organisations to find and drive the science and technology innovations that will grow the UK-economy. The authors would like to thank the team at SAMS for allowing them to conduct the tests at their facilities.

325

## References

- Bard, A.J. and Faulkner, L.R.: Electrochemical Methods: Fundamentals and Applications, Wiley, 2<sup>nd</sup> Ed., ISBN: 978-0-471-04372-0, December 2000.
- Barker, S. and Ridgwell, A.: Nature education: Ocean acidification: [Ocean Acidification | Learn Science at Scitable](https://www.nature.com/subjects/ocean-acidification) (nature.com), 2012. Last access: 17 October 2021.
- 330 Bennett, J. (NOAA): Ocean acidification: [Ocean Acidification | Smithsonian Ocean \(si.edu\)](https://ocean.fishbase.org/ocean-acidification/), April 2018. Last access: 17 October 2021.
- Botnen, H.A., Omar, A.M., Thorseth, I., Johannessen, T. and Alendal, G.: The effect of submarine CO<sub>2</sub> vents on seawater: Implications for detection of subsea carbon sequestration leakage, Limnol. and Oceanogr., 60, 402-410, doi:10.1002/lno.10037, 2015.
- 335 Bresnahan Jr, P.J., Martz, T.R., Takeshita, Y., Johnson, K.S. and LaShomb, M.: Best practices for autonomous measurement of seawater pH with the Honeywell Durafet, Methods in Oceanography, 9, 44,60, doi:10.1016/j.mio.2014.08.003, 2014.
- Briggs, E.M., Sandoval, S., Erten, A., Takeshita, Y., Kummel, A.C., and Martz, T.R.: Solid State Sensor for Simultaneous Measurement of total Alkalinity and pH of Seawater, ACS Sens., 2, 9, 1302-1309, doi:10.1021/acssensors.7b00305, 2017.
- 340 Caldeira, K. and Wicket, M.E.: Ocean model predictions of chemistry changes from carbon dioxide emissions to the atmosphere and ocean, Journal of Geophysical Research: Oceans, C9, 110, doi:10.1029/2004JC002671, 2005.
- Chen, H., Wang, X., Song, X., Zhou, T., Jiang, Y. and Chen, X.: Colorimetric optical pH sensor production using a dual-color system, Sensors and Actuators B, 146, 278-282, doi:10.1016/j.snb.2010.01.068, 2010.
- Chloride Ion Selective Electrodes for pH Measurements in Seawater, Anal. Chem., 86, doi:10.1021/ac502631z, 2014.
- 345 Clayton, T.D. and Byrne, R.H.: Spectrophotometric seawater pH measurement: total hydrogen ion concentration scale calibration of m-cresol purple and at-sea results, Deep Sea Res. Part I: Oceanogr. Res. Pap., 40, 10, 2115-2129, doi:10.1016/0967-0637(93)90048-8, 1993.
- Dai, C., Crawford, L.P., Song, P., Fisher, A.C. and Lawrence, N.S.: A novel sensor based on electropolymerized substituted-phenols for pH detection in unbuffered systems, RSC Adv., 5, 104048-104053, doi:10.1039/c5ra22595g, 2015.

- 350 Dai, C., Song, P., Wadhawan, J.D., Fisher, A.C., and Lawrence, N.S.: Screen Printed Alizarin-Based Carbon Electrodes: Monitoring pH in Unbuffered Media, *Electroanalysis*, 27, 917-923, doi:10.1002/elan.201400704, 2015.
- DeGrandpre, M.D., Spaulding, R.S., Newton, J.O., Jaqueth, E.J., Hamblock, S.E., Umansky, A.A. and Harris, K.E.: Considerations for the measurement of spectrophotometric for ocean acidification and other studies, *Limnol. Oceanogr. Methods*, 12, 12, 830-839, doi:10.4319/lom.2014.12.830, 2014.
- 355 Doney, S.C., Fabry, V.J., Feely, R.A. and Kleypas, J.A.: Ocean acidification: the other CO<sub>2</sub> problem, *Ann Rev Mar Sci.*, 1, 169-92, doi:10.1146/annurev.marine.010908.163834, 2009.
- Downing, J.A.: Limnology and oceanography: two estranged twins reuniting by global change, 4, 215-232, doi:10.5268/IW-4.2.753, 2014.
- Fabry, V.J., Seibel, B.A., Feely, R.A. and Orr, J.C.: Impacts of ocean acidification on marine fauna and ecosystem processes, *ICES Journal of Marine Sci*, 65, 414-432, doi:10.1093/icesjms/fsn048, 2008.
- 360 Hickin, E.J.: River geomorphology, Wiley, New York, 1995.
- Jimenez-Jorquera, C., Orozco, J. and Baldi, A.: ISFET Based Microsensors for Environmental Monitoring, *Sensors*, 10, 61-83, doi:10.3390/s100100061, 2010.
- Johnson, K.S., Jannasch, H.W., Coletti, L.J., Elrod, V.A., Martz, T.R., Takeshita, Y., Carlson, R.J., and Connery, J.G.: Deep-Sea DuraFET: A Pressure tolerant pH Sensor Designed for Global Sensor Networks, *Anal. Chem.*, 88, 6, 3249-3256, doi:10.1021/acs.analchem.5b04653, 2016.
- 365 Kounaves, S.: Chapter 37 Voltammetric Techniques, in: *Handbook of Instrumental Techniques for Analytical Chemistry*, Tufts University, Massachusetts, 709-725, 2008.
- Kremesti, R.E.: Glass pH electrodes vs ISFET pH Electrodes: [Glass pH electrode vs ISFET pH Electrode \(kremesti.com\)](http://kremesti.com). Last access: 21 October 2021.
- 370 Lu, M. and Compton, R. G.: Voltammetric pH sensing using carbon electrodes: glassy carbon behaves similarly to EPPG, *Analyst*, 139, 4599, doi:10.1039/c4an00866a, 2014.
- Martz, T.R., Daly, K.L., Byrne, R.H., Stillman, J.H. and Turk, D.: Technology for Ocean Acidification Research, *Oceanogr.*, 28, 40-47, doi:10.5670/oceanog.2015.30, 2015.
- 375 Martz, T.R., Gonnerly, J.G. and Johnson, S.: Testing the Honeywell Durafet® for seawater pH applications, *Limnol Oceanogr. Methods*, 8, 172-184, doi:10.4319/lom.2010.8.172, 2010.
- Miranda Mugica M., Carveta, C., Sisodia, N., Shirley, L., Day, C.D., McGuinness, K.L., Wadhawan, J.D., and Lawrence, N.S.: Nafion® coated electropolymerized Flavanone-based pH sensor, *Electroanalysis*, 1-8, doi:10.1002/elan.202100652, 2022.
- 380 Miranda Mugica M., McGuinness, K.L. and Lawrence, N.L.: Electropolymerised pH insensitive Salicylic acid reference systems: utilization in a novel pH sensor for food and environmental monitoring, *Sensors*, 22, 1-12, doi:10.3390/s22020555, 2022.

- Newhall, K., Krishfield, R., Peters, D. and Kemp, J.: Deployment Operation Procedures for the WHOI Ice-Tethered Profiler, Technical report, Woods Hole Oceanographic Institution Woods Hole, MA, 41 pp., 2007.
- 385 Oban: Tydes and solunar charts: [Tide times and charts for Oban, Scotland and weather forecast for fishing in Oban in 2021 \(tides4fishing.com\)](https://tides4fishing.com). Last access: 30 October 2021.
- Ocean acidification: [Ocean acidification | National Oceanic and Atmospheric Administration \(noaa.gov\)](https://oceanic.noaa.gov), 1 April 2020. Last access: 17 October 2021.
- pH – SeaBed: [PH – Seabed](https://seabed.com). Last access: 20 October 2021.
- 390 Rerolle, V.M.C., Floquet, C.F.A., Harris, A.J.K., Mowlem, M.C., Bellerby, R.R.G.J. and Achterberg, E.P.: Development of a colorimetric microfluidic pH sensor for autonomous seawater measurements, *Analytica Chimica Acta*, 786, 124-131, doi:10.1016/j.aca.2013.05.008, 2013.
- Rerolle, V.M.C., Ruiz-Pino, D., Rafinadeh, M., Loucaides, S., Papadimitriou, S., Mowlem, M. and Chen, J.: Measuring pH in the Arctic Ocean: Colorimetric method or SeaFET?, *Methods in Oceanogr.*, 17, 32-49, doi:10.1016/j.mio.2016.05.006,
- 395 2016.
- Sabine, C.L., Feely, R.A., Gruber, N., Key, R.M., Lee, K., Bullister, J.L., Wanninkhof, R., Wong, C. S., Wallace, D. W. R., Tilbrook, B., Millero, F.J., Peng, T.H., Kozyr, A., Ono, T. and Rios, A.F.: The oceanic sink for anthropogenic CO<sub>2</sub>, *Science*, 305:5682, 367-71, doi:10.1126/science.1097403, 2004.
- Seidel, M.P., DeGrandpre, M.D. and Dickson, A.G.: A sensor for in situ indicator-based measurement of seawater pH, *Marine Chemistry*, 109, 18-28, doi: 10.1016/j.marchem.2007.11.013, 2008.
- 400 Shitashima, K., Kyo, M., Koike, Y. and Henmi, H.: Development of in situ pH sensor using ISFET, IEEE 2002 International Symposium on Underwater Technology - Tokyo, Japan, doi:10.1109/UT.2002.1002403, 2002.
- Siegenthaler, U., Monnin, E., Kawamura, K., Spahni, R., Schwander, J., Stauffer, B., Stocker, T.F., Barnola, J.M. and Fischer, H.: Supporting evidence from the EPICA Dronning Maud Land ice core for atmospheric CO<sub>2</sub> changes during the past
- 405 millennium, 57:1, 51-57, doi:10.3402/tellusb.v57i1.16774, 2017.
- Sisodia, N., McGuinness, K.L., Wadhawan, J.D, Lawrence, N.S.: In situ recalibration of ion selective electrodes, *Sens. Diagn.*, 1, 134-138, doi:10.1039/D1SD00003A, 2022.
- Stone, M.: Antarctica's ice: <https://www.nationalgeographic.com/environment/article/antarcticas-ice-could-cross-this-scary-threshold-within-40-years>, 5 May 2021. Last access: 10 March 2022.
- 410 Takeshita, Y., Martz, T.R., Johnson, K.S. and Dickson, A.G.: Characterization of an Ion Sensitive Field Effect Transistor and Underwater measurement solutions: [Sea & Sun Technology - Multiparameter Probes \(sea-sun-tech.com\)](https://sea-sun-tech.com). Last access: 20 October 2021.
- Hancock, L.: Why are glaciers and sea ice melting?: <https://www.worldwildlife.org/pages/why-are-glaciers-and-sea-ice-melting>. Last access: 10 March 2022.
- 415 Why pH is important?: [Why pH is important? \(aperainst.com\)](https://aperainst.com), 15 November 2017. Last access: 17 October 2021.